PHYSICAL REVIEW B **76**, 100402(R) (2007)

Non-Fermi-liquid behavior in nearly ferromagnetic $SrIrO_3$ single crystals

G. Cao,[1] V. Durairaj,[1] S. Chikara,[1] L. E. DeLong,[1] S. Parkin,[2] and P. Schlottmann[3]
[1]*Department of Physics and Astronomy, University of Kentucky, Lexington, Kentucky 40506, USA*
[2]*Department of Chemistry, University of Kentucky, Lexington, Kentucky 40506, USA*
[3]*Physics Department, Florida State University, Tallahassee, Florida 32306, USA*
(Received 28 June 2007; revised manuscript received 8 August 2007; published 5 September 2007)

We report magnetic, electric transport, and calorimetric properties of single-crystal $SrIrO_3$ as a function of temperature T and applied magnetic field H. We find that $SrIrO_3$ is a non-Fermi-liquid metal near a ferromagnetic instability, as characterized by the following properties: (1) small saturation moment and no evidence for long-range order down to 1.7 K, (2) strongly enhanced magnetic susceptibility that diverges as T^{γ} at low temperatures with $1/2<\gamma<1$, depending on the applied field, (3) heat capacity $C(T,H)\sim -T\ln T$ that is readily enhanced in low applied fields, and (4) $T^{3/2}$ dependence of electrical resistivity over the range $1.7<T<120$ K. The data imply $SrIrO_3$ is a rare example of a stoichiometric oxide compound that exhibits non-Fermi-liquid behavior near a quantum critical point ($T=0$ and $\mu_0 H=0.23$ T).

DOI: 10.1103/PhysRevB.76.100402 PACS number(s): 75.40.−s, 74.20.Mn, 74.25.Ha

The discoveries of exotic ground states [*p*-wave superconductivity, non-Fermi liquid (NFL)][1,2] in layered ruthenates have inspired extensive investigations on 4*d* and 5*d* materials. Typified by their extended 5*d* orbitals, it is commonly expected that iridates should be more metallic and less magnetic than their 3*d*, 4*d*, and 4*f* counterparts, because of the broader 5*d* bandwidth and the weaker exchange interaction U, so that $Ug(E_F)<1$, where $g(E_F)$ is the density of states at the Fermi energy. However, in marked contrast to these expectations, most of the known iridates, such as layered $BaIrO_3$ (Refs. 3–7) and $Sr_{n+1}Ir_nO_{3n+1}$ ($n=1$ and 2),[8–14] are insulators exhibiting weak ferromagnetism.[15] On the other hand, the layered 4*d* ruthenate analogs ($BaRuO_3$, Sr_2RuO_4, and $Sr_3Ru_2O_7$) are metallic or even superconducting. Although the layered iridates order at relatively high temperatures ($T_c=175$, 240, and 285 K for $BaIrO_3$, Sr_2IrO_4, and $Sr_3Ir_2O_7$, respectively), they attain only a small fraction of the expected ordered moment ($\mu_{or}=0.03$, 0.14, and $0.037\mu_B$/Ir, respectively).[6,12,14] The iridates exhibit strong phase transition signatures in magnetization but none of their T_c's and resistivities are very sensitive to high magnetic fields.[6,12,14] Although a metallic state does not commonly occur in the iridates, the unusual circumstances cited above almost guarantee that it will exhibit extraordinary properties when it does occur. In this paper, we report anomalous transport and thermodynamic properties of single-crystal $SrIrO_3$, which we find is a NFL metal with a ferromagnetic instability extrapolated to zero temperature at an applied magnetic field $\mu_0 H=0.23$ T.

There are several examples of intriguing quantum phenomena occurring in itinerant-electron materials that are on the borderline between ferromagnetism and paramagnetism,[16–18] e.g., *p*-wave superconductivity in Sr_2RuO_4,[1] superconductivity and ferromagnetism in $ZrZn_2$ (Refs. 19 and 20), and URhGe,[21] a ferromagnetic quantum critical point (QCP) in MnSi under pressure,[22] a metamagnetic transition with QCP end point tuned by a magnetic field in $Sr_3Ru_2O_7$,[2] and QCP with anomalous ferromagnetism in $Sr_4Ru_3O_{10}$.[23] In numerous Ce, Yb, and U compounds similar phenomena associated with a QCP, but with antiferromagnetic spin fluctuations have been found,[24] leading to the breakdown of Fermi liquid behavior, including a divergent specific heat [$C/T\sim -\ln T$] and unusual power laws in resistivity ρ and magnetic susceptibility χ at low temperatures.[25,26] The QCP can be tuned by "control parameters" such as composition, pressure, magnetic field, etc.[24–26] To our knowledge $SrIrO_3$ is the first stoichiometric metallic 5*d* system with a nearby QCP that can be readily tuned with very modest magnetic fields; such a rare combination makes $SrIrO_3$ a unique and desirable model system for studies of quantum criticality both experimentally and theoretically.

The crystal structure of $SrIrO_3$ is a monoclinic distortion of the hexagonal $BaTiO_3$ structure[27] with space group $C2/c$ (No. 15) having lattice parameters $a=5.604$ Å, $b=9.618$ Å, $c=14.170$ Å, and $\beta=93.26°$. It features a distorted six-layer hexagonal (6*H*) structure that consists of close-packed Sr-O layers stacked perpendicular to the c axis in the sequence hcchcc, where h and c refer to hexagonal and cubic stacking.

Single crystals were grown in Pt crucibles using self-flux techniques from off-stoichiometric quantities of IrO_2, $SrCO_3$, and $SrCl_2$. Technical details are described elsewhere.[14] The single crystals are of $0.4\times0.4\times0.6$ mm^3 in size. The crystal structure was determined from a small fragment ($0.05\times0.05\times0.05$ mm^3) using Mo$K\alpha$ radiation and a Nonius Kappa CCD single-crystal diffractometer and it is found to be stoichiometric and perfectly consistent with that published in Ref. 27. The composition of the crystals was examined by energy-dispersive x-ray (EDX) spectroscopy, confirming the ratio of Sr:Ir to be 1:1 and uniform. All results indicate high quality of the single crystals without any evidence of impurity. Heat capacity measurements were performed with a Quantum Design PPMS that utilizes a thermal-relaxation calorimeter operating in fields up to 9 T. Magnetic and transport properties were measured using a Quantum Design MPMS 7T LX SQUID magnetometer equipped with a Linear Research Model 700 ac bridge.

Figure 1(a) shows the dc magnetic susceptibility χ as a function of T at $\mu_0 H=0.5$ T for $\mathbf{H}\|\mathbf{c}$ axis (χ_c) and $\mathbf{H}\perp\mathbf{c}$ axis (χ_{ab}). Both χ_c and χ_{ab} are clearly temperature dependent and large, particularly for $T<15$ K. In contrast, IrO_2 is a Pauli

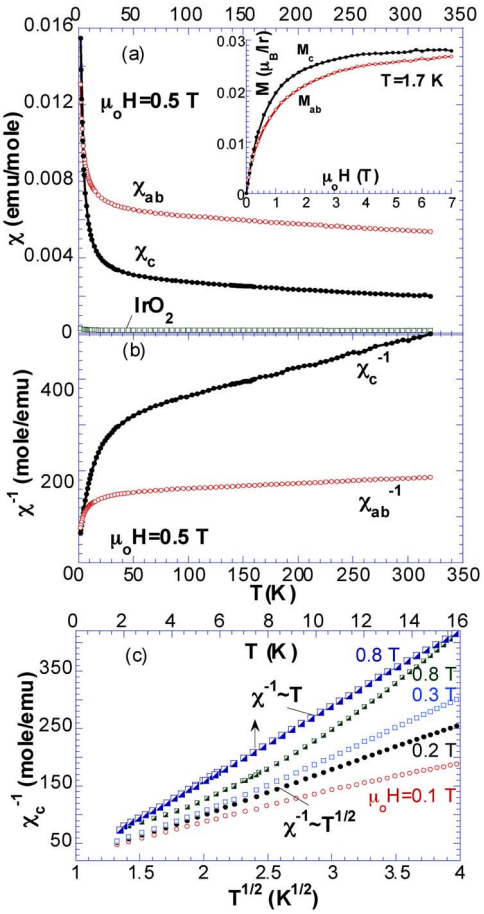

FIG. 1. (Color online) (a) The magnetic susceptibility χ as a function of temperature at $\mu_0 H=0.5$ T for $H\|\mathbf{c}$ axis (χ_c) and $H\perp\mathbf{c}$ axis (χ_{ab}). χ for polycrystalline IrO_2 is also shown for comparison. Inset: Isothermal magnetization M vs H at $T=1.7$ K. (b) Reciprocal susceptibility χ_c^{-1} and χ_{ab}^{-1} as a function of temperature for $\mu_0 H=0.5$ T. (c) χ_c^{-1} as a function of $T^{1/2}$ and T (upper scale, for $B=0.8$ T marked by an arrow). The behavior of χ_{ab}^{-1} is similar and not shown.

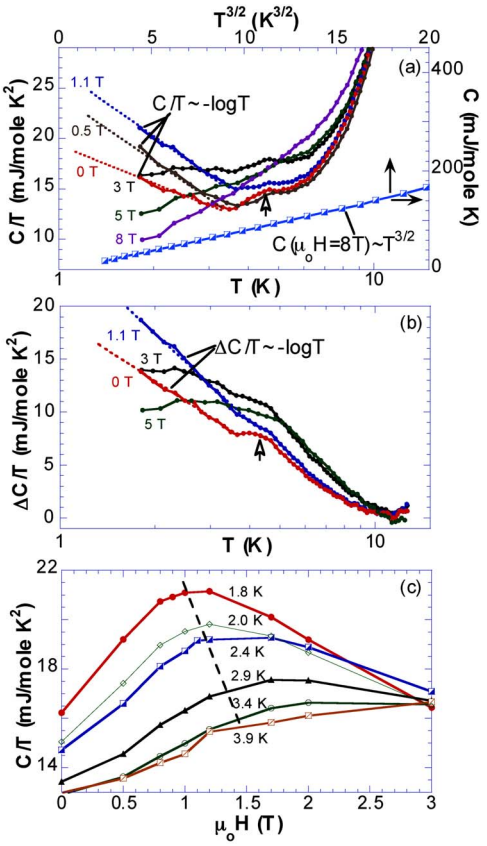

FIG. 2. (Color online) (a) The specific heat C divided by temperature C/T vs $\ln T$ for $\mu_0 H=0$, 0.5, 1.1, 3, 5, and 8 T and C vs $T^{3/2}$ (right and upper scales) for $\mu_0 H=8$ T. (b) $\Delta C/T$ vs $\ln T$ (see definition of ΔC in text) for $\mu_0 H=0$, 1.1, 3, 5 T. (c) C/T vs H for some representative temperatures.

paramagnet with a much smaller, temperature-independent χ ($\sim 10^{-4}$ emu/mole Ir), which indicates a significant exchange enhancement $Ug(E_F)$ is present in $SrIrO_3$ ($>10^{-3}$ emu/mole Ir). The sharp rise below 15 K suggests the proximity to a ferromagnetic instability although χ shows no sign of saturation at 1.7 K. (Note that χ_c surpasses χ_{ab} at $T<5$ K.) Indeed, the isothermal magnetization $M(H)$ at $T=1.7$ K is already saturated at $\mu_0 H\sim 3$ T, as seen in the inset to Fig. 1(a). It needs to be pointed out that $M(H)$ follows no Brillouin function although it appears Brillouin-like. On the other hand, the saturation moment μ_{sat} is less than 3% of that expected ($1\mu_B$/Ir) for an $S=1/2$ system and decreases with increasing T, which is indicative of a nearby Stoner instability.

The reciprocal susceptibilities χ_c^{-1} and χ_{ab}^{-1} display linear T dependences, consistent with a Curie-Weiss behavior for $T>120$ K, as shown in Fig. 1(b). However, the Curie-Weiss fits of the data for both $\mu_0 H=0.1$ (not shown) and 0.5 T yield effective moments and Curie-Weiss temperatures that are much too large to be physically meaningful. This behavior is similar to that observed for the exchange-enhanced paramagnet $SrRhO_3$.[28,29] Moreover, for $1.7<T<15$ K, χ_c^{-1} and χ_{ab}^{-1} follow non-standard power laws that range from $T^{1/2}$ for $\mu_0 H<0.3$ T to linear T for $\mu_0 H>0.8$ T, as shown in Fig. 1(c). Relevantly, $M(H)$ remains essentially linear below 0.6 T (see the inset). This high sensitivity of the temperature exponent to low applied magnetic fields again suggests the rapid approach to a ferromagnetic instability although the ground state is yet to be more conclusively determined via further measurements at the milli-Kelvin range.

The low-temperature specific heat $C(T,H)$ data acquired over $1.8<T<24$ K and $\mu_0 H<8$ T offer important insights into the low-energy excitations of $SrIrO_3$. For $T>12$ K, the specific heat is well described by $C(T)=\gamma T+\beta T^3$ with $\gamma=1.50$ mJ/mole K^2 and $\beta=0.28$ mJ/mole K^4, yielding a Debye temperature of 326 K, and suggesting that only electronic and phonon contributions are significant in this temperature range (data not shown). The small γ value implies that renormalizations of the effective mass are insignificant above 12 K and/or there is only a small area on the Fermi surface.

The heat capacity data exhibit intriguing temperature and field dependences below 13 K, as shown in Fig. 2(a), where C/T vs T is plotted for $1.8<T<12.8$ K. A broad shoulder is observed near 4.5 K, which weakens with increasing field

and eventually vanishes at $\mu_0 H > 3$ T. The field dependence suggests a magnetic mechanism, but $\chi(T,H)$ shows no corresponding transition. This broad peak in C/T is followed at lower temperatures by a pronounced $\ln(T)$ dependence, characteristic of NFL systems,[19] and suggests a vanishing Fermi temperature ($T_F \to 0$) and a divergent quasiparticle effective mass ($m^*/m \to \infty$). It is clear that the amplitude of the logarithmic term rapidly grows with increasing field until $\mu_0 H = 1.1$ T, where it becomes weaker, and eventually vanishes for $\mu_0 H > 2$ T. C/T slowly drops off with decreasing $T < 6$ K for $\mu_0 H > 3$ T, which suppress magnetic fluctuations and lead to the recovery of Fermi-liquid behavior. This crossover is accompanied by a strengthening of magnetic correlations at fields approaching 8 T, as illustrated in Fig. 2(a), which shows that $C(T,H)$ evolves from the NFL $T\ln(T)$ behavior to a $T^{3/2}$ power law expected for magnon excitations out of a ferromagnetically ordered state.

The magnetic contribution to the heat capacity ΔC at low temperatures is obtained by subtracting the electronic (γT) and phonon (βT^3) contributions that dominate $C(T)$ in the range $10 < T < 24$ K. The plot of $\Delta C/T$ vs T shown in Fig. 2(b) emphasizes the logarithmic behavior of $\Delta C/T$ for $B = 0$ and 1.1 T for $T < 10$ K. The strong enhancement of $\Delta C/T$ with only weak applied fields < 1.5 T reflects the growth of quantum critical fluctuations near a ferromagnetic instability. The strong competition between a ferromagnetic state and spin fluctuations can be inferred from the intermingling of the $\ln T$ dependence and the hump in $\Delta C/T$ located near 4.5 K,which, for $\mu_0 H = 3$ and 5 T, broadens as the low-temperature, singular behavior of $\Delta C/T$ disappears.

The detailed field dependence of C/T reveals two interesting features shown for representative isotherms in Fig. 2(c). (1) C/T peaks at a critical field H_c that separates a regime for $H < H_c$ where $C/T \sim -\ln(T)$ increases with H, from the complementary regime for $H > H_c$ where the $\ln(T)$ dependence weakens and eventually disappears. The peak fades and C/T becomes much less field dependent for $T > 4$ K. On the basis of the $C(T,H)$ data an H-T phase diagram [Fig. 3(a)] can be constructed to reveal a linear increase of H_c with temperature that can be extrapolated to $T = 0$ K to locate the QCP at $\mu_0 H_c = 0.23$ T. (2) All C/T curves converge at $\mu_0 H = 3$ T. This is unlikely to be a coincidence, as $\mu_0 H = 3$ T clearly renders C/T temperature independent [see Fig. 2(a)] and $M(H)$ becomes saturated near 3 T (see Fig. 1). An ongoing analysis of the data suggests a complex scaling behavior associated with this characteristic field.

It is also worth mentioning that the Wilson ratio $R_W \equiv 3\pi^2 k_B^2 \chi/\mu_B^2 \gamma$, is 74.96 at $T = 1.8$ K and shows weak temperature dependence below 3 K, as shown in Fig. 3(b). This strikingly large R_W is clearly the consequence of non-Fermi-liquid behavior, and far beyond the values (e.g., $R_W \sim 1-6$) typical of heavy Fermi liquids and exchange-enhanced paramagnets such as Pd.[30] But R_W drops rapidly at $T > 3$ K, where the C/T peak fades [see Fig. 3(a)], reaffirming the crossover to Fermi-liquid behavior [see Fig. 3(b)].

The presence of the quantum critical fluctuations is further corroborated by the temperature dependence of the **c** axis ρ_c and **ab** plane ρ_{ab} resistivities as a function of T, shown in Fig. 4(a). The residual resistivity ρ_0 is 2.2 $\mu\Omega$ cm and 0.66 mΩ cm for ρ_{ab} and ρ_c, respectively, and the residual resistance ratio (RRR) ≈ 3. An interesting feature is that ρ_c and ρ_{ab} exhibit a $T^{3/2}$ law over a wide temperature range up to 120 K, which is particularly strong for ρ_c, as

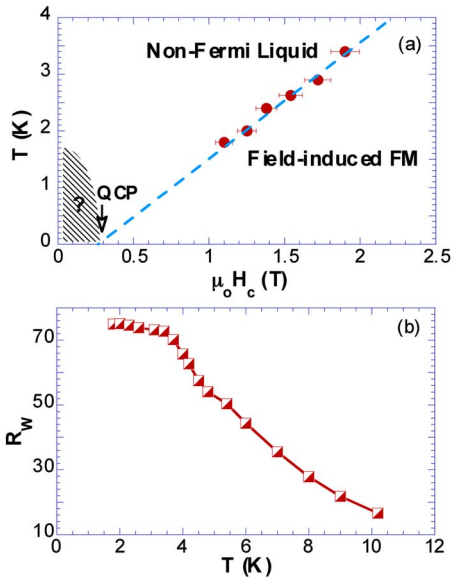

FIG. 3. (Color online) (a) An H-T phase diagram generated based on the data in Fig. 2. The dashed line is a guide to the eye. (b) The Wilson ratio R_W as a function of T. R_W is estimated based on χ and C/T at $\mu_0 H = 0.5$ T.

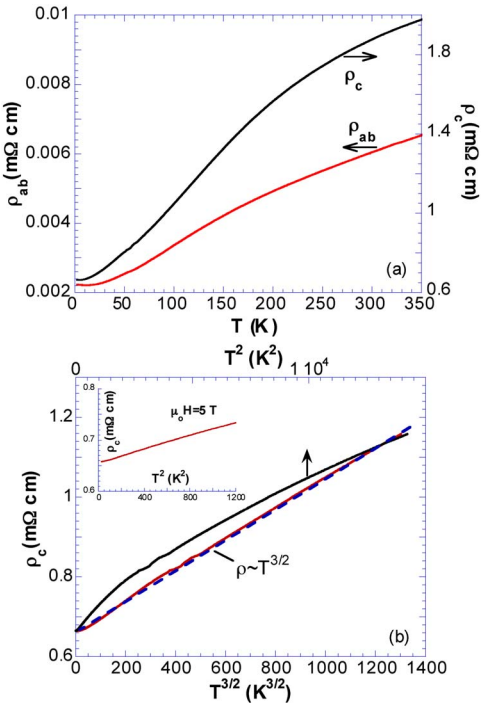

FIG. 4. (Color online) (a) The basal plane and c-axis resistivity, ρ_{ab} and ρ_c (right scale) as a function of temperature. (b) ρ_c vs $T^{3/2}$ and T^2 (upper scale) for $1.7 < T < 120$ K at $\mu_0 H = 0$ T. Inset: ρ_c vs T^2 for $1.7 < T < 37$ K at $\mu_0 H = 5$ T.

shown in Fig. 4(b), where ρ_c vs T^2 (upper scale) is also shown for comparison. At $\mu_0 H \geq 5$ T, the temperature dependence of ρ changes from $T^{3/2}$ to T^2 (see inset), suggesting a recovery of Fermi-liquid behavior. It is remarkable that ρ exhibits a large anisotropy ($\rho_c/\rho_{ab} \sim 300$) that is essentially temperature independent, implying quasi-two-dimensional transport, although the magnetic susceptibility is much less anisotropic, suggesting three-dimensional magnetic correlations.

The $T^{3/2}$ and $T^{5/3}$ laws are seen in QCP systems such as MnSi,[25] $Sr_3Ru_2O_7$,[2] $Sr_4Ru_3O_{10}$,[23,31] and some heavy-fermion systems.[25] The $T^{5/3}$ dependence is attributed to dominant low-angle electron scattering by low-q spin fluctuations,[25] hence weakening the temperature dependence of the resistivity from T^2. The power-law $T^{3/2}$ is thought to be associated with effects of diffusive electron motion caused by strong interactions between itinerant electrons and critically damped very-long-wavelength magnons.[19]

It is compelling to ascribe the non-Fermi-liquid behavior in $SrIrO_3$ to proximity to a QCP given the phase diagram and the observed physical properties that are dominated by strong spin fluctuations. This first study on single-crystal $SrIrO_3$ reveals it to be a stoichiometric oxide with unusual sensitivity to low magnetic fields, which makes it an outstanding model system for studies of quantum criticality. In light of the phase diagram of Fig. 3(a) and the association of weak ferromagnetism with triplet-paired superconductivity near a QCP, it is urgent to explore the physical properties of $SrIrO_3$ in the milli-K range and at high pressures.

G. C. would like to thank Dr. W. Crummett for useful discussions. This work was supported by NSF through Grant No. DMR-0240813 and 0552267. P. S. is supported by the DOE through Grant No. DE-FG02-98ER45707.

[1] Y. Maeno, H. Hashimoto, K. Yoshida, S. Nishizaki, T. Fujita, J. G. Bednorz, and F. Lichtenberg, Nature (London) **372**, 532 (1994).
[2] S. A. Grigera, R. P. Perry, A. J. Schofield, M. Chiao, S. R. Julian, G. G. Lonzarich, S. I. Ikeda, Y. Maeno, A. J. Millis, and A. P. Mackenzie, Science **294**, 329 (2001).
[3] T. Siegrist and B. L. Chamberland, J. Less-Common Met. **170**, 93 (1991).
[4] A. V. Powell and P. D. Battle, J. Alloys Compd. **191**, 313 (1993).
[5] R. Lindsay, W. Strange, B. L. Chamberland, and R. O. Moyer, Solid State Commun. **86**, 759 (1993).
[6] G. Cao, J. E. Crow, R. P. Guertin, P. Henning, C. C. Homes, M. Strongin, D. N. Basov, and E. Lochner, Solid State Commun. **113**, 657 (2000).
[7] G. Cao, X. N. Lin, S. Chikara, V. Durairaj, and E. Elhami, Phys. Rev. B **69**, 174418 (2004).
[8] M. K. Crawford, M. A. Subramanian, R. L. Harlow, J. A. Fernandez-Baca, Z. R. Wang, and D. C. Johnston, Phys. Rev. B **49**, 9198 (1994).
[9] D. C. Johnston, T. Ami, F. Borsa, M. K. Crawford, J. A. Fernandez-Baca, K. H. Kim, R. L. Harlow, A. V. Mahajan, L. L. Miller, M. A. Subramanian, D. R. Torgeson, and Z. R. Wang, in *Spectroscopy of Mott Insulators and Correlated Metals*, edited by A. Fujimori and Y. Tokura (Springer, Berlin, 1995), p. 249.
[10] Q. Huang, J. L. Soubeyroux, O. Chmaissen, I. Natali Sora, A. Santoro, R. J. Cava, J. J. Krajewski, and W. F. Peck, Jr., J. Solid State Chem. **112**, 355 (1994).
[11] R. J. Cava, B. Batlogg, K. Kiyono, H. Takagi, J. J. Krajewski, W. F. Peck, Jr., L. W. Rupp, Jr., and C. H. Chen, Phys. Rev. B **49**, 11890 (1994).
[12] G. Cao, J. Bolivar, S. McCall, J. E. Crow, and R. P. Guertin, Phys. Rev. B **57**, R11039 (1998).
[13] S. J. Moon, M. W. Kim, K. W. Kim, Y. S. Lee, J.-Y. Kim, J.-H. Park, B. J. Kim, S.-J. Oh, S. Nakatsuji, Y. Maeno, I. Nagai, S. I. Ikeda, G. Cao, and T. W. Noh, Phys. Rev. B **74**, 113104 (2006).
[14] G. Cao, Y. Xin, C. S. Alexander, J. E. Crow, P. Schlottmann, M. K. Crawford, R. L. Harlow, and W. Marshall, Phys. Rev. B **66**, 214412 (2002).
[15] Magnetism in spin chains with geometric frustration has been recently observed in insulating $Ca_5Ir_3O_{12}$ and Ca_4IrO_6, for example, G. Cao, V. Durairaj, S. Chikara, S. Parkin, and P. Schlottmann, Phys. Rev. B **75**, 134402 (2007).
[16] L. E. De Long, J. G. Huber, and K. S. Bedell, J. Magn. Magn. Mater. **99**, 171 (1991).
[17] G. Cao, S. McCall, J. E. Crow, and R. P. Guertin, Phys. Rev. Lett. **78**, 1751 (1997).
[18] X. N. Lin, Z. X. Zhou, V. Durairaj, P. Schlottmann, and G. Cao, Phys. Rev. Lett. **95**, 017203 (2005).
[19] C. Pfleiderer, M. Uhlarz, S. M. Hayden, R. Vollmer, H. von Lohneysen, N. R. Bernhoeft, and G. G. Lonzarich, Nature (London) **412**, 58 (2001).
[20] E. A. Yelland, S. M. Hayden, S. J. C. Yates, C. Pfleiderer, M. Uhlarz, R. Vollmer, H. v. Löhneysen, N. R. Bernhoeft, R. P. Smith, S. S. Saxena, and N. Kimura, Phys. Rev. B **72**, 214523 (2005), in which the superconductivity is reported to be caused by effects of spark erosion.
[21] D. Aoki, A. Huxley, E. Ressouche, D. Braithwaite, J. Floquet, J. P. Brison, E. Lhotel, and C. Paulsen, Nature (London) **413**, 613 (2001).
[22] C. Pfleiderer, S. R. Julian, and G. G. Lonzarich, Nature (London) **414**, 427 (2001).
[23] G. Cao, S. Chikara, J. W. Brill, and P. Schlottmann, Phys. Rev. B **75**, 024429 (2007).
[24] For example, G. R. Stewart, Rev. Mod. Phys. **73**, 797 (2001).
[25] M. B. Maple, Physica B **215**, 110 (1995).
[26] M. B. Maple, M. C. de Andrade, J. Herrmann, Y. Dalichaouch, D. A. Gajewski, C. L. Seaman, R. Chau, R. Movshovich, M. C. Aronson, and R. Osborn, J. Comput. Phys. **99**, 223 (1995).
[27] J. M. Longo, J. A. Kafalas, and R. J. Arnott, J. Solid State Chem. **3**, 174 (1971).
[28] K. Yamaura and E. Takayama-Muromachi, Phys. Rev. B **64**, 224424 (2001).
[29] D. J. Singh, Phys. Rev. B **67**, 054507 (2003).
[30] L. E. DeLong, R. P. Guertin, S. Hasanain, and T. Fariss, Phys. Rev. B **31**, 7059 (1985).
[31] S. Chikara, V. Durairaj, W. H. Song, Y. P. Sun, X. N. Lin, A. Douglass, G. Cao, P. Schlottmann, and S. Parkin, Phys. Rev. B **73**, 224420 (2006).